

Gas-phase nitronium ion affinities

F. CACACE*†, G. DE PETRIS†‡, F. PEPI*, AND F. ANGELELLI*

*Dipartimento di Studi di Chimica e Tecnologia delle Sostanze Biologicamente Attive, Università degli Studi di Roma "La Sapienza," Piazzale Aldo Moro, 5, 00185 Rome, Italy; and †Dipartimento di Scienze Ambientali, Università della Tuscia, v. S. C. De Lellis, 01100 Viterbo, Italy

Communicated by Alfred P. Wolf, Brookhaven National Laboratory, Upton, NY, April 24, 1995

ABSTRACT Evaluation of nitronium ion-transfer equilibria, $L_1\text{NO}_2^+ + L_2 = L_2\text{NO}_2^+ + L_1$ (where L_1 and L_2 are ligands 1 and 2, respectively) by Fourier-transform ion cyclotron resonance mass spectrometry and application of the kinetic method, based on the metastable fragmentation of $L_1(\text{NO}_2^+)L_2$ nitronium ion-bound dimers led to a scale of relative gas-phase nitronium ion affinities. This scale, calibrated to a recent literature value for the NO_2^+ affinity of water, led for 18 ligands, including methanol, ammonia, representative ketones, nitriles, and nitroalkanes, to absolute NO_2^+ affinities, that fit a reasonably linear general correlation when plotted vs. the corresponding proton affinities (PAs). The slope of the plot depends to a certain extent on the specific nature of the ligands and, hence, the correlations between the NO_2^+ affinities, and the PAs of a given class of compounds display a better linearity than the general correlation and may afford a useful tool for predicting the NO_2^+ affinity of a molecule based on its PA. The NO_2^+ binding energies are considerably lower than the corresponding PAs and well below the binding energies of related polyatomic cations, such as NO^+ , a trend consistent with the available theoretical results on the structure and the stability of simple NO_2^+ complexes. The present study reports an example of extension of the kinetic method to dimers, such as $L_1(\text{NO}_2^+)L_2$, bound by polyatomic ions, which may considerably widen its scope. Finally, measurement of the NO_2^+ affinity of ammonia allowed evaluation of the otherwise inaccessible PA of the amino group of nitramide and, hence, direct experimental verification of previous theoretical estimates.

The study of the complexes formed in the gas phase by NO_2^+ is currently the focus of considerable fundamental interest (1–11) and, in addition, has a direct bearing on areas ranging from mechanistic organic chemistry (12–19) to atmospheric chemistry, clustering and nucleation phenomena, intracuster reactivity (20–30), etc. In view of the considerable interest of the problem and of the scant experimental information currently available (31–33), we have undertaken a systematic study of the binding energy (BE) of NO_2^+ to representative ligands, aimed at the construction of a gas-phase nitronium ion-affinity scale.

To this end, we have applied the Fourier-transform ion cyclotron resonance mass spectroscopy equilibrium method largely used in proton affinity (PA) measurements (34) to NO_2^+ transfer reactions and extended the kinetic method, so far used exclusively in PA and gas-phase acidity determinations (35, 36), to nitronium ion-bound dimers.

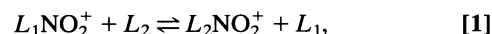
MATERIALS AND METHODS

All chemicals were obtained as research-grade products from Aldrich and were used without further purification. The gases were purchased from Matheson with a stated purity >99.95 mol %, except NO_2 , for which purity was >99.5 mol %, and were used

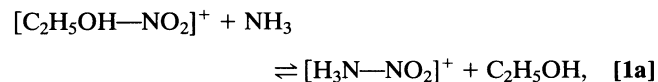
without further purification. The mass analyzed ion kinetic energy (MIKE) spectra were recorded using a ZAB-2F mass spectrometer from VG Analytical (Manchester, U.K.), whose chemical ionization source was fitted with a specially built device, designed to cool the source block, removing the heat radiated from the filament by a stream of cold N_2 . The spectra were recorded at temperatures ranging from 40° to 50°C, as measured by a thermocouple inserted into the source block, using gaseous mixtures of NO_2 and the two ligands (L_1 and L_2), whose composition was optimized to obtain the highest intensity of the $L_1(\text{NO}_2^+)L_2$ dimers, at total pressures in the 0.1- to 0.5-torr (1 torr = 133 Pa) range. Typical experimental conditions were as follows: electron energy, 50 eV (1 eV = 1.602×10^{-19} J); repeller voltage, 0 V; emission current, 0.5 mA; accelerating voltage, 8 kV. Each MIKE spectrum represents the average of at least 20 scans, with an energy resolution of 2000 full width at half-maximum (fwhm). The equilibrium measurements were done by using a Bruker (Billerica, MA) Spectrospin Apex TM 47e Fourier transform ion cyclotron resonance mass spectrometer, equipped with an external chemical ionization source and an XMASS TM Bruker data system. To prevent errors due to the different response of the ionization manometer to different compounds, premixed gaseous mixtures, obtained by weighted amounts of the reactants, were used.

RESULTS

Fourier Transform Ion Cyclotron Resonance Equilibrium Measurements. Evaluation of ligand exchange equilibria,



allows direct determination of the corresponding free energy change, ΔG_1^\ddagger , provided that the equilibrium constant can be accurately measured, which requires attainment of true equilibrium, unperturbed by significant side reactions. In the specific application, $\text{CH}_3\text{O}(\text{NO}_2)_2^+$, the nitrating reagent, is prepared in the external chemical ionization source of a Fourier transform ion cyclotron resonance mass spectrometer and driven into the resonance cell, where it nitrates both ligands, present in a known concentration ratio. One of the nitrated complexes is isolated by selective-ejection techniques and allowed to equilibrate in the mixture of the ligands. Application of the method is prevented in many cases by incursion of fast proton-transfer reactions that perturb the equilibrium—e.g., the nitronium ion transfer,



undergoes competition by proton transfer to ammonia from both nitrated complexes, which react as the conjugate acids of ethyl nitrate and of nitramide. Furthermore, in the case of ligands of low ionization potential the study of equilibrium 1

The publication costs of this article were defrayed in part by page charge payment. This article must therefore be hereby marked "advertisement" in accordance with 18 U.S.C. §1734 solely to indicate this fact.

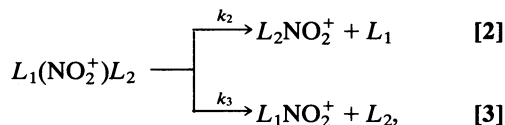
Abbreviations: PA, proton affinity; BE, binding energy; RP, reference pair; MIKE, mass analyzed ion kinetic energy.

†To whom reprint requests should be addressed.

is adversely affected by competing charge-transfer reactions. As a consequence, application of the equilibrium method is restricted to those systems where proton- and/or electron-transfer processes are sufficiently slower than reaction 1, as in the example illustrated in Fig. 1. In most cases, equilibrium 1 could be attained from both sides, and the ΔG_1° changes reported in Table 1 are the mean values of sets of at least three measurements, performed at different $[L_1]/[L_2]$ ratios, characterized by SDs appreciably lower than the $\pm 0.1 \text{ kcal}\cdot\text{mol}^{-1}$ (1 cal = 4.184 J) uncertainty quoted, which reflects instead a conservative estimate of the errors affecting the $[L_1]/[L_2]$ ratio, the measurement of the ionic intensities, etc.

The Kinetic Method. The limitations of the equilibrium method have suggested extension to nitronium ion-bound dimers of the kinetic method developed by Cooks and co-workers (35, 36) for proton-bound dimers and subsequently applied to alkali cation-bound dimers (37) and other metal cation-bound clusters (38–41). It is a limiting procedure, based on several nonrigorous assumptions that nevertheless has proved highly successful in a variety of applications, especially in those systems where weakly bound dimers undergo simple dissociation kinetics, which is the case of many nitronium ion-bound dimers (see below).

In the case of interest, application of the kinetic method is based on the MIKE spectrometry of $L_1(\text{NO}_2^+)L_2$ nitronium ion-bound dimers, obtained by $\text{NO}_2/\text{chemical}$ ionization of gaseous mixtures of the ligands. The conceivable formation of clusters—e.g., proton-bound dimers of the same m/z ratio but structurally different from nitronium ion-bound dimers—has required preliminary selection of the species suitable for application of the kinetic method. Fortunately a systematic survey has allowed identification of many $(L_1, L_2, \text{NO}_2)^+$ clusters whose metastable fragmentation occurs exclusively via the competing processes



suggesting that the dissociating species has the structure of a $L_1(\text{NO}_2^+)L_2$ nitronium ion-bound dimer, as in the representative examples illustrated in Fig. 2. Adopting the same set of

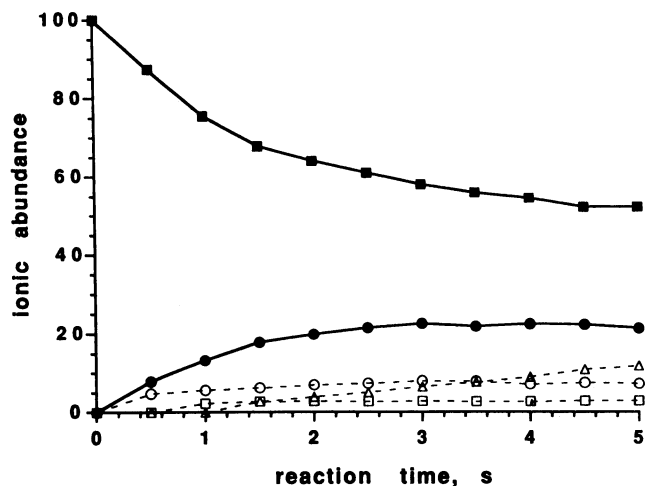


FIG. 1. Time dependence of the relative ionic abundances of $\text{CH}_3\text{CN}\cdot\text{NO}_2^+$ (■) and $(\text{CH}_3)_2\text{CO}\cdot\text{NO}_2^+$ (●) ions in a 5.65:1 $\text{CH}_3\text{CN}/(\text{CH}_3)_2\text{CO}$ mixture at a total pressure of $5.0\cdot 10^{-8}$ torr (uncorrected). Other ions are as follows: $[(\text{CH}_3)_2\text{CO}]\text{H}^+$ (△), NO_2^+ (○), and $(\text{CH}_3\text{CN})\text{H}^+$ (□).

Table 1. ΔG° changes from the equilibrium and the kinetic method

L_1	L_2	$-\Delta G_{300}^\circ, \text{ kcal}\cdot\text{mol}^{-1}$ *	
		Equilibrium method	Kinetic method
H_2O	CH_3OH	1.9†	RP‡
H_2O	$\text{CH}_2(\text{CN})_2$	2.1	
CH_3OH	CH_3NO_2		1.3
CH_3NO_2	$\text{C}_2\text{H}_5\text{NO}_2$	1.4	1.1
$\text{C}_2\text{H}_5\text{NO}_2$	CH_3CN	1.6	1.3
CH_3CN	CH_3COCH_3	0.5	0.6
$\text{C}_2\text{H}_5\text{NO}_2$	CH_3COCH_3	1.9	1.8
CH_3COCH_3	$\text{C}_2\text{H}_5\text{CN}$	0.5	0.6
CH_3CN	$\text{C}_2\text{H}_5\text{CN}$	0.9	1.2
CH_3COCH_3	$\text{CH}_3\text{COC}_2\text{H}_5$	0.8	RP
$\text{C}_2\text{H}_5\text{CN}$	$\text{CH}_3\text{COC}_2\text{H}_5$		0.5
$\text{CH}_3\text{COC}_2\text{H}_5$	$i\text{-C}_3\text{H}_7\text{CN}$		0.2
$\text{C}_2\text{H}_5\text{CN}$	$i\text{-C}_3\text{H}_7\text{CN}$	0.7	RP
CH_3COCH_3	$i\text{-C}_3\text{H}_7\text{CN}$	1.2	RP
CH_3CN	$i\text{-C}_3\text{H}_7\text{CN}$	1.5	RP
$i\text{-C}_3\text{H}_7\text{CN}$	$(\text{C}_2\text{H}_5)_2\text{O}$	0.2	RP
$\text{C}_2\text{H}_5\text{CN}$	$(\text{C}_2\text{H}_5)_2\text{O}$	0.5	0.8
CH_3COCH_3	$(\text{C}_2\text{H}_5)_2\text{O}$	1.1	
CH_3CN	$(\text{C}_2\text{H}_5)_2\text{O}$	1.4	
$(\text{C}_2\text{H}_5)_2\text{O}$	NH_3		0.2
$i\text{-C}_3\text{H}_7\text{CN}$	NH_3		0.2
CH_3COCH_3	NH_3		1.0
$i\text{-C}_3\text{H}_7\text{CN}$	$\text{C}_6\text{H}_5\text{CN}$	0.5	0.4
$\text{CH}_3\text{COC}_2\text{H}_5$	$\text{C}_6\text{H}_5\text{CN}$		0.6
$\text{C}_6\text{H}_5\text{CN}$	$(\text{C}_2\text{H}_5)_2\text{CO}$		0.1
$(\text{C}_2\text{H}_5)_2\text{O}$	$(\text{C}_2\text{H}_5)_2\text{CO}$	0.5	
$i\text{-C}_3\text{H}_7\text{CN}$	$(\text{C}_2\text{H}_5)_2\text{CO}$		0.4
$\text{CH}_3\text{COC}_2\text{H}_5$	$(\text{C}_2\text{H}_5)_2\text{CO}$	0.8	0.5
$(\text{C}_2\text{H}_5)_2\text{CO}$	$t\text{-C}_4\text{H}_9\text{COCH}_3$		0.3
$t\text{-C}_4\text{H}_9\text{COCH}_3$	$(i\text{-C}_3\text{H}_7)_2\text{CO}$		0.8
$(\text{C}_2\text{H}_5)_2\text{CO}$	$(i\text{-C}_3\text{H}_7)_2\text{CO}$		1.1
$\text{CH}_3\text{COC}_2\text{H}_5$	$(i\text{-C}_3\text{H}_7)_2\text{CO}$		1.8
$(i\text{-C}_3\text{H}_7)_2\text{CO}$	$\text{C}_6\text{H}_5\text{COCH}_3$		0.3
$t\text{-C}_4\text{H}_9\text{COCH}_3$	$\text{C}_6\text{H}_5\text{COCH}_3$		0.8
$(\text{C}_2\text{H}_5)_2\text{CO}$	$\text{C}_6\text{H}_5\text{COCH}_3$		1.3
$\text{C}_6\text{H}_5\text{COCH}_3$	$(\text{C}_6\text{H}_5)_2\text{CO}$		0.8

L , ligand; $i\text{-C}_3\text{H}_7$, isopropyl; $t\text{-C}_4\text{H}_9$, *tert*-butyl.

*Accuracy of data is discussed in text.

†Data are from ref. 10.

‡RP denotes a reference pair used for construction of the calibration plot.

assumptions and approximations customarily used in the case of proton-bound dimers, one obtains the expression

$$\ln\left(\frac{i(L_2\text{NO}_2^+)}{i(L_1\text{NO}_2^+)}\right) = \ln\left(\frac{k_2}{k_3}\right) = \frac{-\partial(\Delta G^\circ)}{RT},$$

where $\partial(\Delta G^\circ) = \Delta G_2^\circ - \Delta G_3^\circ$ corresponds to the ΔG_1° change of the nitronium ion-transfer reaction [1], T represents the "effective" temperature of the dimers that undergo observable metastable fragmentation, and i is the intensity of the charged fragments. In practice, the appropriate value of T is deduced from the slope of a calibration plot constructed using a set of independently measured ΔG° values. To this end, six pairs of ligands, henceforth denoted as RPs, have been selected, whose $L_1(\text{NO}_2^+)L_2$ dimers undergo intense and clean metastable decompositions and whose ΔG_1° changes had been measured by the equilibrium method. The plot of $\ln(k_2/k_3)$ vs. the known $\delta(\Delta G^\circ)$ values of the six RPs is characterized by an excellent linearity (correlation coefficient, 0.9987) and a negligible intercept. From the plot one obtains $T = 225 \text{ K}$, which has been used to evaluate the ΔG_1° changes listed in Table 1, together

with the corresponding ΔG_{300}° changes from the equilibrium method. Comparison of the two sets of values, excluding of course the six RPs, shows that the differences do not exceed 0.3 kcal·mol⁻¹, their mean value being as low as 0.2 kcal·mol⁻¹.

Whereas neither approach allows direct measurement of free energy changes >2 kcal·mol⁻¹, the individual ΔG_1° changes for all pairs of ligands can be combined to construct a ladder that spans the entire range investigated, some 10 kcal·mol⁻¹ (Fig. 3). Under the assumption that $\Delta G_1^{\circ} \cong \Delta H_1^{\circ}$, such a fixed-temperature free energy scale approximates a relative BE scale, which has been anchored to the independently known H₂O—NO₂⁺ BE, 19.6 ± 2.4 kcal·mol⁻¹, according to earlier equilibrium measurements (10) in close agreement with the value of 20.1 kcal·mol⁻¹ (at 298 K) from a high-level *ab initio* study (8) to obtain the absolute BE values listed in Table 2.

The internal consistency of the ΔG_1° ladder, strengthened by multiple interlacing of its steps, is <0.1 kcal·mol⁻¹, increasing to 0.2 kcal·mol⁻¹ only for the pairs including NH₃. A larger uncertainty is introduced by taking $\Delta G_1^{\circ} \cong \Delta H_1^{\circ}$, a practice widely adopted in the derivation of PAs from single-temperature equilibrium data (34). A rough estimate of the error involved can be based on the recent evaluation of 80 proton-transfer equilibria (42), characterized by a mean ΔS° change of 3.6 ± 2.2 cal·K⁻¹, whose neglect would introduce a 1.1 kcal·mol⁻¹ mean error into the corresponding ΔH_{300}° values. In this connection, it should be noted that the only independently known ΔS_1° change, which refers to the H₂O/CH₃OH pair (10), amounts to -2.7 ± 1 cal·K⁻¹·mol⁻¹, corresponding to a $\Delta H_1^{\circ} - \Delta G_1^{\circ}$ difference of 0.8 kcal·mol⁻¹ at 300 K. Last, but not least, one must take into account the uncertainty arising from the error bar of ±2.4 kcal·mol⁻¹ attached to the H₂O—NO₂⁺ BE used as the reference value. Overall, the absolute uncertainty of the individual BE values is estimated to amount to ±2.6 kcal·mol⁻¹, and their internal consistency is estimated at ±1.3 kcal·mol⁻¹.

DISCUSSION

A concise survey of the structure of the complexes formed in the gas phase by NO₂⁺ is of interest. A suitable model of the

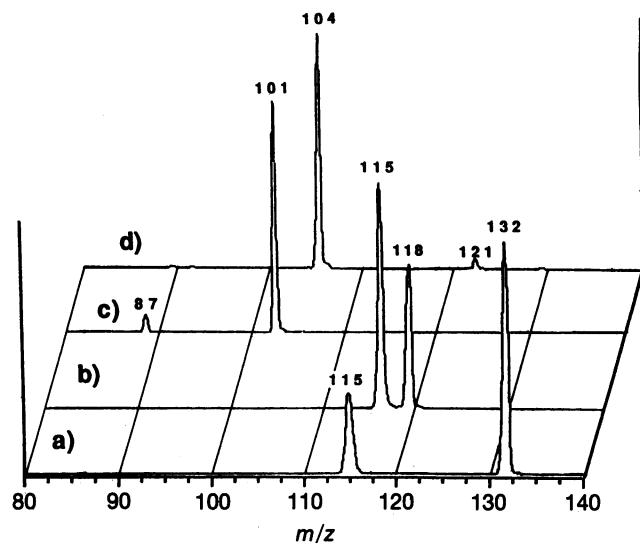


FIG. 2. Representative MIKE spectra of nitronium ion-bound dimers. Spectra: a, (C₂H₅)₂CO(NO₂⁺)*i*-C₃H₇CN (where *i*-C₃H₇ is isopropyl), giving *i*-C₃H₇CN·NO₂⁺, $m/z = 115$, and (C₂H₅)₂CO·NO₂⁺, $m/z = 132$; b, *i*-C₃H₇CN(NO₂⁺)CH₃COC₂H₅, giving *i*-C₃H₇CN·NO₂⁺, $m/z = 115$, and CH₃COC₂H₅·NO₂⁺, $m/z = 118$; c, C₂H₅CN(NO₂⁺)·CH₃CN, giving CH₃CN·NO₂⁺, $m/z = 87$, and C₂H₅CN·NO₂⁺, $m/z = 101$; d, C₂H₅NO₂(NO₂⁺)(CH₃)₂CO giving (CH₃)₂CO·NO₂⁺, $m/z = 104$, and C₂H₅NO₂·NO₂⁺, $m/z = 121$. In each spectrum the intensities are normalized to the most intense peak.

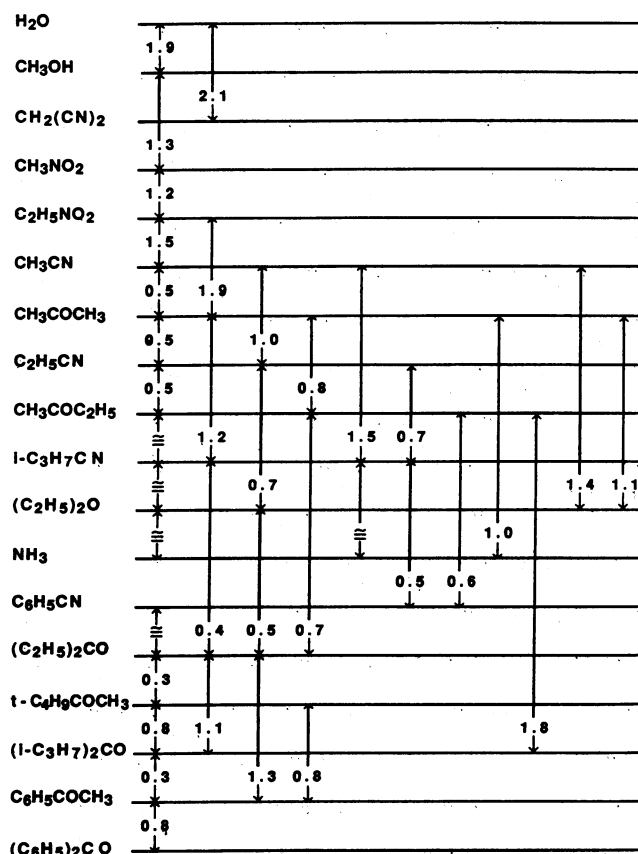


FIG. 3. ΔG° ladder for NO₂⁺ transfer reactions for different ligand pairs. The steps correspond to the mean between the results from the kinetic method and those from the equilibrium method when both data are available for a given reaction. As to the accuracy of the results, see text. The \cong symbol indicates values ≤ 0.2 kcal·mol⁻¹.

complexes containing a single ligand molecule is the most stable isomer of protonated nitric acid, which, according to the results of high-level *ab initio* calculations, is best described as an ion-molecule complex, H₂O—NO₂⁺, characterized by a large separation, 2.50 Å, and a minor deformation of the mono-

Table 2. NO₂⁺ BEs of selected ligands, L

No.	L	BE, kcal·mol ⁻¹ *
1	H ₂ O	19.6 [†]
2	CH ₃ OH	21.5
3	CH ₂ (CN) ₂	21.7
4	CH ₃ NO ₂	22.8
5	C ₂ H ₅ NO ₂	24.0
6	CH ₃ CN	25.5
7	CH ₃ COCH ₃	25.9
8	C ₂ H ₅ CN	26.5
9	CH ₃ COC ₂ H ₅	26.8
10	<i>i</i> -C ₃ H ₇ CN	27.0
11	(C ₂ H ₅) ₂ O	27.1
12	NH ₃	27.2
13	C ₆ H ₅ CN	27.5
14	(C ₂ H ₅) ₂ CO	27.6
15	<i>t</i> -C ₄ H ₉ COCH ₃	27.9
16	(<i>i</i> -C ₃ H ₇) ₂ CO	28.7
17	C ₆ H ₅ COCH ₃	29.0
18	(C ₆ H ₅) ₂ CO	29.8

L, ligand; *i*-C₃H₇, isopropyl; *t*-C₄H₉, *tert*-butyl.

*Accuracy of data is discussed in text.

[†]Data are from ref. 10.

mers—e.g., the O—N—O angle of the nitro group of the complex is computed to be 177° vs. the 180° angle of the free NO_2^+ (6). The IR spectrum of gaseous $\text{H}_2\text{O}-\text{NO}_2^+$ displays two bands assigned to H_2O stretching, whose maxima differ by $<50\text{ cm}^{-1}$ from those of H_2O . These, and other spectroscopic features, point to a distant and relatively weak coordination of the monomers in the $\text{H}_2\text{O}-\text{NO}_2^+$ complex (27, 30), consistent with the theoretical results. The same picture is outlined by *ab initio* studies of the gaseous complexes formed by NO_2^+ with HClO (24) and CH_3OH (8) and of the complexes containing two ligands—e.g., the $\text{H}_2\text{O}-(\text{NO}_2^+)-\text{OH}_2$ cation (7), characterized as a weakly bound complex, consistent with the evidence from IR and photodissociation spectroscopy (27, 30). In summary, the available structural evidence underlines the reluctance of the nitronium ion to form tightly bound complexes undergoing the necessary structural changes, in particular as concerns the deformation of its geometry.

Data Correlation and Analysis. In general, the NO_2^+ BEs are much smaller than the corresponding PAs, which reflects the fact that the electrostatic energy release due to the charge expansion from the small H^+ to the larger LH^+ ion exceeds, at any given separation, that due to the charge expansion from the NO_2^+ ion to the LNO_2^+ complex. Furthermore, the cation–ligand separation is much smaller in the case of H^+ than of NO_2^+ , characterized by a distant coordination with the nucleophile, as discussed in the previous paragraph.

Including all the ligands investigated (Table 2, no. 1–18), one obtains the plot presented in Fig. 4, for which least-squares analysis gives the correlation NO_2^+ BE = $-18.89 + 0.231\text{ PA}$, where the energies are expressed in $\text{kcal}\cdot\text{mol}^{-1}$. Although reasonably linear (correlation coefficient = 0.9688), the plot allows only a rough estimate of the NO_2^+ BE of a compound, based on its PA. The limitation reflects the composite character of the plot because the correlation between the NO_2^+ BE and the PA differs for different classes of compounds, as illustrated in Fig. 5 for ketones and nitriles, showing that when a single class of compounds is considered, the linearity of the plots improves considerably, and their slopes can afford a more useful tool for predicting NO_2^+ BEs.

Comparison of the BE of NO_2^+ with that of other polyatomic cations is also of interest. We shall restrict the comparison to a closely related cation, the nitrosonium ion NO^+ , whose BEs to selected ligands have been reported by Reents and Freiser (43). In general, the NO^+ BEs are considerably larger than the corresponding NO_2^+ BEs, owing, in part, to the smaller size, and hence higher charge density, of NO^+ than of NO_2^+ . However, the paramount factor is probably to be found in the much smaller ion–ligand separation in the NO^+ complexes.

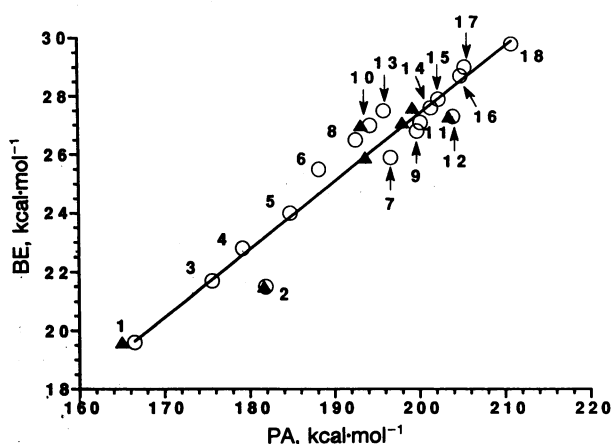


FIG. 4. General correlation between NO_2^+ BEs and PA values from ref. 34 (○). When available, the PA values from the recently reevaluated scale of ref. 42 (▲) are included for comparison.

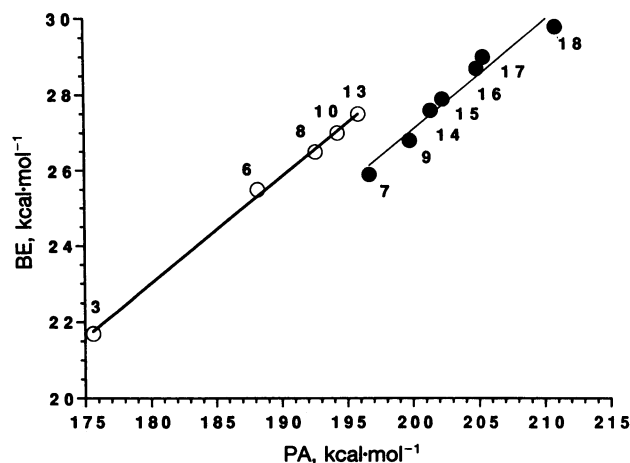


FIG. 5. Correlation between NO_2^+ BEs and PAs for specific classes of compounds: ketones (●) and nitriles (○).

According to a recent *ab initio* study (44), the monomer separation amounts to 2.20 \AA in the $\text{H}_2\text{O}-\text{NO}^+$ complex vs. the $2.50\text{-}\text{\AA}$ separation in the $\text{H}_2\text{O}-\text{NO}_2^+$ complex, which entails a considerably smaller electrostatic stabilization of the latter. Furthermore, at variance with NO_2^+ , NO^+ does not appear to undergo energetically unfavorable structural deformation upon complexation—e.g., the N—O equilibrium bond length does not change significantly in passing from free NO^+ to its complex with water (44).

In summary, comparison of the NO_2^+ and NO^+ BEs, as well as of the extent of structural changes undergone by the two cations upon complexation, points to the reluctance of nitronium ion to form tightly bound complexes, characterized by a small separation between the nucleophilic center and the cation and by a significant deformation of the latter. Such a behavior is in line with the large reorganization energy of the initially linear NO_2^+ cation to a bent structure, identified by Ebersson and Radner (45) as a major component of the activation energy for aromatic nitration in solution.

Local PAs of Nitramide. The results of this study allow experimental verification of the theoretical predictions concerning the relative basicity of the NH_2 and the NO_2 groups of nitramide. According to a recent *ab initio* study (31), nitramide is an oxygen base in the gas phase, and its experimental PA = $182.1 \pm 2\text{ kcal}\cdot\text{mol}^{-1}$ refers to protonation at the nitro group, whereas the local PA of the amino group amounts to $175.0\text{ kcal}\cdot\text{mol}^{-1}$, which corresponds to a $\text{H}_3\text{N}-\text{NO}_2^+$ BE of $27\text{ kcal}\cdot\text{mol}^{-1}$. The agreement with the experimental values from this work, 175.4 and $27.2\text{ kcal}\cdot\text{mol}^{-1}$, respectively, is excellent, although such a degree of consistency is partially fortuitous, owing to the significant error bars attached to both sets of results.

Extension of the Kinetic Method to Dimers Bound by Polyatomic Ions. Comparison with the results from the equilibrium method shows that the kinetic method, when applied to $(\text{L}_1, \text{L}_2, \text{NO}_2)^+$ clusters whose metastable fragmentation occurs exclusively according to processes 2 and 3, performs beyond expectations, despite the problems anticipated when dealing with a polyatomic binding ion, whose structure and vibrational frequencies may change considerably, and to a different extent, along the reaction coordinates of the competitive dissociation processes 2 and 3. This change may render the method less accurate than in applications involving the monoatomic, structureless binding ions, such as H^+ and Li^+ , used in all previous studies. The present results indicate that, at least in the case of NO_2^+ , the problem is less vexing than anticipated, probably due to the specific, singularly favorable properties of the nitronium ion.

The financial support from the Italian Ministero per l'Università e la Ricerca Scientifica e Tecnologica (MURST) and Consiglio Nazionale delle Ricerche (CNR) is gratefully acknowledged.

1. Fehsenfeld, F. C., Howard, C. J. & Schmeltekopf, A. L. (1975) *J. Chem. Phys.* **63**, 2835–2841.
2. Nguyen, M.-T. & Hegarty, A. F. (1984) *J. Chem. Soc. Perkin Trans. 2*, 2043–2045.
3. Cacace, F., Attinà, M., de Petris, G. & Speranza, M. (1990) *J. Am. Chem. Soc.* **112**, 1014–1018.
4. de Petris, G. (1990) *Org. Mass Spectrom.* **25**, 83–86.
5. Bernardi, F., Cacace, F. & Grandinetti, F. (1989) *J. Chem. Soc. Perkin Trans. 2*, 413–415.
6. Lee, T. J. & Rice, J. E. (1992) *J. Phys. Chem.* **96**, 650–657.
7. Grandinetti, F., Bencivenni, L. & Ramondo, F. (1992) *J. Phys. Chem.* **96**, 4354–4358.
8. Lee, T. J. & Rice, J. E. (1992) *J. Am. Chem. Soc.* **114**, 8247–8256.
9. Sunderlin, L. S. & Squires, R. R. (1993) *Chem. Phys. Lett.* **212**, 307–311.
10. Cacace, F., Attinà, M., de Petris, G. & Speranza, M. (1994) *J. Am. Chem. Soc.* **116**, 6413–6417.
11. Ricci, A. (1994) *Org. Mass Spectrom.* **29**, 55–56.
12. Politzer, P., Jayasuriya, K., Sjöberg, P. & Laurence, P. R. (1985) *J. Am. Chem. Soc.* **107**, 1174–1177.
13. Feng, J., Zhang, X. & Zerner, M. C. (1986) *J. Org. Chem.* **51**, 4531–4536.
14. Gleghorn, J. T. & Torossian, G. (1987) *J. Chem. Soc. Perkin Trans. 2* 1303–1310.
15. Sandall, J. P. B. (1992) *J. Chem. Soc. Perkin Trans. 2*, 1689–1693.
16. Szabó, K. J., Hörnfeldt, A.-B. & Gronowitz, S. (1992) *J. Am. Chem. Soc.* **114**, 6827–6834.
17. Bernardi, F., Robb, M. A., Rossi, I. & Venturini, A. (1993) *J. Org. Chem.* **58**, 7074–7078.
18. Attinà, M., Cacace, F. & Speranza, M. (1992) *Int. J. Mass Spectrom. Ion Processes* **117**, 37–46.
19. Aschi, M., Attinà, M., Cacace, F. & Ricci, A. (1994) *J. Am. Chem. Soc.* **116**, 9535–9542.
20. Fehsenfeld, F. C. & Ferguson, E. E. (1969) *J. Geophys. Res.* **74**, 2217–2222.
21. Brasseur, G. & Solomon, S. (1986) *Aeronomy of the Middle Atmosphere* (Riedel, Dordrecht, The Netherlands).
22. Boehringer, H., Fahey, D. W., Fehsenfeld, F. C. & Ferguson, E. E. (1983) *Planet Space Sci.* **31**, 185–191.
23. Nelson, C. M. & Okumura, M. (1992) *J. Phys. Chem.* **96**, 6112–6115.
24. Lee, T. J. & Rice, J. E. (1993) *J. Phys. Chem.* **97**, 6637–6644.
25. Kay, B. D., Hermann, V. & Castleman, A. W., Jr. (1981) *Chem. Phys. Lett.* **80**, 469–474.
26. Horn, A. B., Koch, T., Chester, M. A., McCoustra, M. R. S. & Sodeaw, J. R. (1994) *J. Phys. Chem.* **98**, 946–951.
27. Cao, Y., Choi, J.-H., Haas, B.-M., Johnson, M. S. & Okumura, M. (1993) *J. Chem. Phys.* **99**, 9307–9309.
28. Zhang, X., Mereand, E. L. & Castleman, A. W., Jr. (1994) *J. Phys. Chem.* **98**, 3554–3557.
29. Stace, A. J., Winkel, J. F. & Atrill, S. R. (1994) *J. Chem. Soc. Faraday Trans. 90*, 3469–3470.
30. Cao, Y., Choi, J.-H., Haas, B.-M. & Okumura, M. (1994) *J. Phys. Chem.* **98**, 12176–12185.
31. Attinà, M., Cacace, F., Ciliberto, E., de Petris, G., Grandinetti, F., Pepi, F. & Ricci, A. (1993) *J. Am. Chem. Soc.* **115**, 12398–12404.
32. Schulz, W., Drost, H. & Klotz, H. D. (1968) *Org. Mass Spectrom.* **1**, 391–395.
33. Izod, T. P. J. & Tedder, J. M. (1974) *Proc. R. Soc. London A* **337**, 333–350.
34. Lias, S. G., Bartmess, J. E., Liebman, J. F., Holmes, J. L. & Mallard, W. G. (1988) *J. Phys. Chem., Suppl.* **1**.
35. McLuckey, S. A., Cameron, D. & Cooks, R. G. (1981) *J. Am. Chem. Soc.* **103**, 1313–1317.
36. Majumdar, T. K., Clairet, F., Tabet, J. C. & Cooks, R. G. (1992) *J. Am. Chem. Soc.* **114**, 2897–2903.
37. Puzo, G., Fournié, J. J. & Promé, J. C. (1985) *Anal. Chem.* **57**, 892–894.
38. Fournié, J. J. & Puzo, G. (1985) *Anal. Chem.* **57**, 2287–2289.
39. Puzo, G., Promé, J. C. & Fournié, J. J. (1985) *Carbohydr. Res.* **140**, 131–134.
40. Jarrold, M. F., Bower, J. E. & Kraus, J. S. (1987) *J. Chem. Phys.* **86**, 3876–3885.
41. Isa, K. & Takeuchi, Y. (1989) *Org. Mass Spectrom.* **24**, 153–156.
42. Szulejko, J. E. & McMahon, T. B. (1993) *J. Am. Chem. Soc.* **115**, 7839–7848.
43. Reents, W. D., Jr., & Freiser, B. S. (1981) *J. Am. Chem. Soc.* **103**, 2791–2797.
44. de Petris, G., Di Marzio, A. & Grandinetti, F. (1991) *J. Phys. Chem.* **95**, 9782–9787.
45. Ebersson, L. & Radner, F. (1984) *Acta Chem. Scand. Ser. B* **38**, 861–870.